Preprint typeset using LaTeX style emulateapj v. 11/12/01

EARLY STAR FORMATION TRACED BY THE HIGHEST REDSHIFT QUASARS

R. MAIOLINO[1], Y. JUAREZ[2], R. MUJICA[2], N. M. NAGAR[3] AND E. OLIVA[1,4]

ABSTRACT

The iron abundance relative to α-elements in the circumnuclear region of quasars is regarded as a clock of the star formation history and, more specifically, of the enrichment by type Ia supernovae (SNIa). We investigate the iron abundance in a sample of 22 quasars in the redshift range 3.0<z<6.4 by measuring their rest frame UV FeII bump, which is shifted into the near-IR, and by comparing it with the MgII λ2798 flux. The observations were performed with a device that can obtain near-IR spectra in the range 0.8–2.4μm in one shot, thereby enabling an optimal removal of the continuum underlying the FeII bump. We detect iron in all quasars including the highest redshift (z=6.4) quasar currently known. The uniform observational technique and the wide redshift range allows a reliable study of the trend of the FeII/MgII ratio with redshift. We find the FeII/MgII ratio is nearly constant at all redshifts, although there is marginal evidence for a higher FeII/MgII ratio in the quasars at z$\sim$6. If the FeII/MgII ratio reflects the Fe/α abundance, this result suggests that the z$\sim$6 quasars have already undergone a major episode of iron enrichment. We discuss the possible implications of this finding for the star formation history at z>6. We also detect a population of weak iron emitters at z$\sim$4.5, which are possibly hosted in systems that evolved more slowly. Alternatively, the trend of the FeII/MgII ratio at high redshift may reflect significantly different physical conditions of the circumnuclear gas in such high redshift quasars.

Subject headings: quasars: emission lines — galaxies: evolution, high-redshift

1. INTRODUCTION

The iron abundance relative to α-elements has been regarded as a clock indicator of the star formation history (e.g. Hamann & Ferland 1999). Indeed most of the iron in local galaxies is thought to be produced by type Ia SNe, while α-elements are predominantly produced by type II SNe. The difference between the progenitor masses of SNIa and SNII (hence in their life times) translates into an enrichment delay between the Fe and α-elements, which was generally thought to be about 1 Gyr (Wheeler, Sneden, & Truran 1989). However, more recent studies have shown that SNIa are also enhanced in young stellar systems (e.g. Mannucci et al. 2003). In particular the SNIa progenitors may be as massive as 8 $M_{\odot}$ (Greggio & Renzini 1983), which have a lifetime of $\sim 3\times10^7$yr. As a consequence the maximum of iron enrichment may occur on relatively short timescales depending on the star formation history and on the initial mass function (Matteucci & Recchi 2001).

The prominent emission lines observed in quasars allow us to investigate the metallicity of galactic nuclei at large cosmological distances (Hamann & Ferland 1999). The main iron feature in quasar spectra is the UV bump at 2200–3090Å, which is the blend of several thousand FeII (and some FeIII) lines. The ratio of the FeII (UV) bump to the MgII λ2798 doublet is sensitive to the Fe/α abundance ratio, but is also sensitive to other physical properties of the emitting region such as microturbulence, density, and ionization parameter (Verner et al. 2003). As a consequence it is not simple to quantitatively derive the Fe/α ratio from the FeII(UV)/MgII ratio alone. The FeII(UV)/MgII ratio can be used as a *relative* indicator of Fe/α among quasars, under the assumption that the physical properties of the emitting regions are the same.

At z>3 the UV iron bump is shifted in the infrared. Several authors have measured the FeII/MgII ratio in high redshift quasars by means of near-IR spectroscopy (Aoki, Murayama, & Denda 2002; Dietrich et al. 2002, 2003; Freudling, Corbin, & Korista 2003; Iwamuro et al. 2002; Thompson, Hill, & Elston 1999). Yet, the main difficulty in several of these studies (with the exception of Dietrich et al. 2002, 2003) is that most infrared instruments can only cover a fraction of the near-IR spectrum in a single observation, and the broad FeII pseudo continuum can well cover the entire observed spectral range, making it very difficult to recover the true underlying continuum.

In this letter the results of the analysis of near-IR spectra of 22 high redshift quasars will be presented. These spectra were obtained with an instrumental setup that can cover the full near-IR spectrum from 0.8μm to 2.4μm in one shot (and with very high throughput), therefore allowing a good estimate of the continuum underlying the FeII bump. Our observations provide a relatively large sample of FeII/MgII measurements over a wide redshift range and obtained with the same technique and fitting method. Therefore these data allow for a reliable investigation of the redshift dependence of the FeII/MgII ratio. Throughout the paper we adopt H_0 = 70 km s^{-1}Mpc^{-1}, Ω_M = 0.3 and Ω_Λ = 0.7.

[1] INAF – Osservatorio Astrofisico di Arcetri, largo E. Fermi 5, 50125 Firenze, Italy; maiolino@arcetri.astro.it

[2] Instituto Nacional de Astrofísica Óptica y Electronica, Puebla, Luis Enrique Erro 1, Tonantzintla, Puebla 72840, Mexico; yjuarez@inaoep.mx, rmujica@inaoep.mx

[3] Kapteyn Institute, University of Groningen, Landleven 12, 9747 AD Groningen, The Netherlands; nagar@astro.rug.nl

[4] Telescopio Nazionale Galileo, Calle Alvarez de Abreu, 70, 38700 Santa Cruz de La Palma, Spain; oliva@tng.iac.es

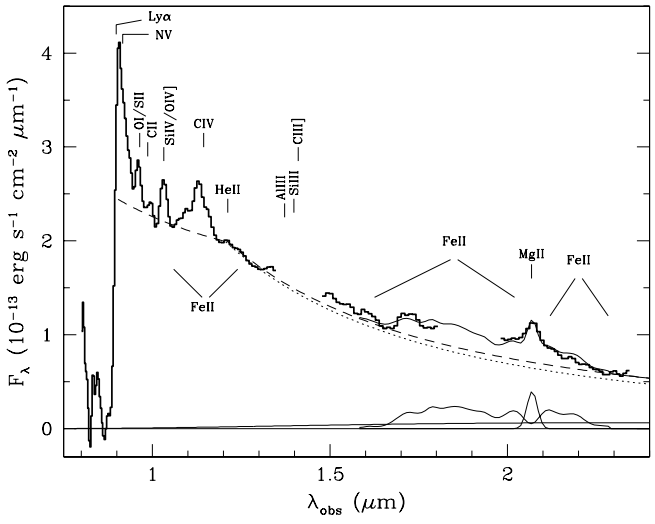

FIG. 1.— Near infrared spectrum of the highest redshift quasar SDSSJ114816.64+525150.3 at z=6.4. The upper thick line shows the observed spectrum, where regions of bad atmospheric transmission have been omitted, while the overimposed thin solid line shows the best fit to the continuum, FeII and MgII, as discussed in the text. The dotted line shows the power-law component ($F_\lambda \propto \lambda^\alpha$, $\alpha = -1.9$), while the dashed line shows the total continuum fit (i.e. by including the Balmer continuum). The lower part of the figure shows the single components of the fit and, more specifically, FeII bump, MgII line and Balmer continuum.

2. OBSERVATIONS

The observations were obtained with the Near Infrared Camera Spectrograph (NICS) at the Italian Telescopio Nazionale Galileo, a 3.56 m telescope. Among the various imaging and spectroscopic observing modes (Baffa et al. 2001), NICS offers a unique, high sensitivity, low resolution observing mode, which uses an Amici prism as a dispersing element (Oliva 2003). In this mode it is possible to obtain the spectrum from 0.8μm to 2.4μm in one shot. The throughput of the Amici prism is nearly two times higher than other more commonly used dispersers. The spectral resolution with a 0″.75 slit, as it was in our case, is 75 (i.e. 4000 km s^{-1}) and nearly constant over the whole wavelength range. This observing mode is appropriate to study the near-infrared continuum of faint sources, and to detect broad ($\sim$ 5000 km s^{-1}) emission lines in faint quasars as well as pseudo-continua such as the FeII bump which require a careful subtraction of the underlying continuum. Observations were performed in three observing runs: 2002 November 7-9; 2003 February 25-29; and 2003 May 23-26. Typical integration times ranged from $\sim$20 minutes, for bright objects, to $\sim$2 hours for faint objects. We include also the data of SDSSJ1044-0125 obtained previously at the same instrument and already published in Maiolino et al. (2001). Several quasars were observed more than once on different nights to check for any instrumental or observational artifacts in the individual spectra. Wavelength calibration was performed by using an argon lamp and the deep telluric absorption features. The telluric absorption was then removed by dividing the quasar spectrum by a reference star spectrum (FV-GV) observed at similar airmass. The intrinsic features and slope of the reference star were then removed by multiplying the corrected quasar spectrum by a spectrum of the same stellar type from the library by Pickles (1998), smoothed to our resolution. Absolute flux calibration was obtained by using the photometry on the acquisition image or through photometry reported in the literature.

In total 22 quasars were observed. These were selected among the brightest (observable during each run) in each of the following redshift ranges: 3.0-3.6, 4.3-5.1, 5.8-6.4, which ensure that the MgII and a good fraction of the FeII are observed outside the deepest atmospheric absorption regions (with the only exception of SDSS1044-0125 at z=5.78 whose MgII is in a bad atmospheric band, but which could be used to derive the average quasars spectrum, see next section).

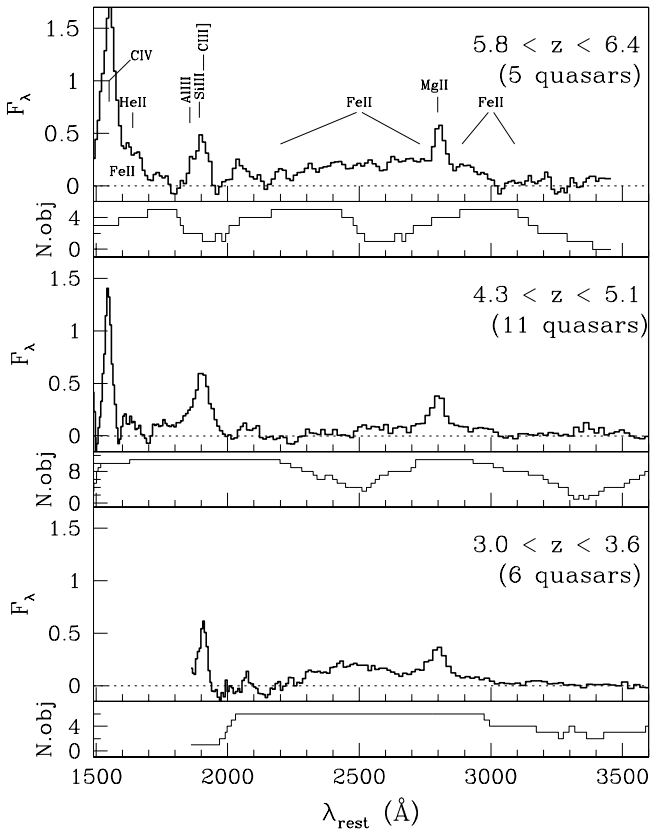

FIG. 2.— Average quasar spectra (residuals after continuum subtraction) around the FeII UV bump obtained by grouping the objects in the three main redshift bins and by normalizing each spectrum to the continuum at the wavelength of MgII. Beneath each panel we also show the number of individual quasar spectra which where used to create the average spectrum. Regions where the number of quasars is low correspond to the spectral segments more seriously affected by the strong atmospheric absorption in that redshift range (see text).

3. DATA ANALYSIS AND FITTING TECHNIQUE

In Fig.1 we show the resulting spectrum of the highest redshift quasar SDSSJ114816.64+525150.3, at z=6.40 (Fan et al. 2003)[5], along with the identification of the major spectral features. Some blue-shift is observed for the CIV line. This shift may be due to an imperfect correction of the atmospheric absorption dip which occurs at the same wavelength; however, Barth et al. (2003) also find the same effect, suggesting that the shift may be real. The spectrum of the highest redshift quasar shows a prominent FeII bump. All the other spectra and the detailed analysis of their spectral features will be presented in a forthcoming paper. Here we focus on the analysis of the UV iron complex and of the MgII λ2798Å blend. The continuum fitting we performed was similar to the method adopted by Dietrich et al. (2002, 2003) and Wills, Netzer, &

[5] The best redshift fitting the observed wavelength of MgII in our spectrum is 6.40, in agreement with the redshift obtained by Willott, McLure, & Jarvis (2003) and Barth et al. (2003).

Wills (1985), i.e. we included both a powerlaw and a Balmer continuum. The continuum was fitted in the spectral regions free of emission features, and away from regions of very bad atmospheric transmission. In Fig.1 we show the power-law ($F_\lambda \propto \lambda^\alpha$, $\alpha = -1.9$) plus Balmer-continuum fit to the spectrum of SDSSJ114816.64+525150.3. Note that in the highest redshift quasars (z>5.8) there is a flattening in the continuum blueward of CIV, that is also observed in the optical spectra of quasars at 3<z<5 (Francis et al. 1991; Vanden Berk et al. 2001), possibly as a consequence of intervening metal absorption lines. At variance with other authors, who prefer to fit the powerlaw by sampling the continuum redward of 3100Å and the continuum between CIV and Lyα (but leaving positive continuum residuals between CIV and FeII), we prefer to fit separately the continuum on either side of CIV with two different power-laws. This also ensures that the continuum fit of the quasars at z>5.8 is consistent with the continuum fit of the lower redshift quasars.

In Fig.2 we show the averages of the quasars residual spectra after continuum subtraction (and normalized to the continuum flux near the MgII line) and grouped in the three main redshift ranges discussed above. In each spectrum the regions of strong atmospheric absorption were discarded, but the spread in redshift allows to cover continuously the whole spectral region around FeII and MgII. Beneath each average spectrum we show the number of quasar spectra which populate each spectral region. While both the low redshift and the high redshift average spectra clearly show a prominent FeII bump, the average of the intermediate redshift quasars is characterized by a significantly lower intensity of the FeII bump (middle panel). This might be partly due to the region at $\lambda < 2500$Å being poorly populated since severe atmospheric absorption separating the J and H bands affects several quasars in this spectral region at these redshifts. However, the FeII emission close to MgII is not affected by this problem. Therefore we believe that the weakness of FeII in the average spectrum of intermediate redshift quasars is real.

The MgII line and the residuals in the region around the FeII bump (2200–3090Å rest frame) were fitted, for each object, by using the Vestergaard & Wilkes (2001) iron template, smoothed to the velocity dispersion of MgII, and a broad gaussian at the wavelength of the MgII line. These fitting components for the case of SDSSJ114816.64+525150.3 are shown in Fig.1. The FeII flux was integrated between the rest-frame wavelengths 2200 and 3090Å. In Table 1 we report the FeII/MgII ratio for all quasars observed by us. We also list the rest-frame luminosity λL_λ at 1450Å (note that thanks to our wide spectral coverage we can measure this quantity directly in several quasars, or by performing only a minor extrapolation).

We note that the continuum and Fe fitting techniques, as well as the instrumental setup, have often been different among previous works on this subject. As a consequence, a comparison of the results between these different studies may be subject to strong uncertainties (although some authors attempt to correct as much as possible for these systemic differences, e.g. Dietrich et al. 2003). Within this context we emphasize that our survey provides uniform and homogeneous FeII/MgII measurements for a set of 22 quasars spanning a wide redshift range (3.0–6.4) obtained with the same instrumental setup (which covers the entire near-IR in one spectrum), same spectral resolution (constant over the whole spectral range) and same fitting technique. Therefore they represent a self-consistent sample which is well suited to study the trend of FeII/MgII with redshift.

Some of the quasars observed by us were also observed by other authors and deserve some comparison, even with the caveats discussed above. BR 2237-0607 and BR 0019-1522 were observed by Dietrich et al. (2003) who find higher FeII/MgII ratios than us, but the inconsistency is not large when errors are taken into account. BR 2237-0607 was also observed by Iwamuro et al. (2002), who obtain a ratio consistent with ours. SDSSJ103027.10+052455.0 was observed with HST/NICMOS by Freudling, Corbin, & Korista (2003) and they derived a much lower value for the FeII/MgII ratio (2.1 ± 1.1) than found by us (8.64 ± 2.47). However, Freudling et al. did not measure MgII directly in this object, but instead estimated the MgII flux from the measured CIII] flux and an assumed CIII]/MgII ratio similar to the average of other quasars. Also, they did not sample the continuum redward of the FeII bump. SDSSJ114816.64+525150.3 was observed by Barth et al. (2003), who found a lower FeII/MgII value (4.7 ± 0.4) than ours, though marginally consistent with errors ($\sim 1.5\sigma$). Their spectral coverage does not extend enough to sample the continuum outside the iron bump, this might have led them to overestimate the underlying continuum.

In Fig.3 we show the average of the FeII/MgII ratios within the three redshift ranges discussed above. In the same figure we also plot the FeII/MgII ratio obtained by Dietrich et al. (2003) from composite optical spectra of quasars at lower redshift matching nearly the same luminosity range as the objects in our sample. No trend of the FeII/MgII with luminosity was found within the luminosity range of our sample, which spans about 1.5 orders of magnitude.

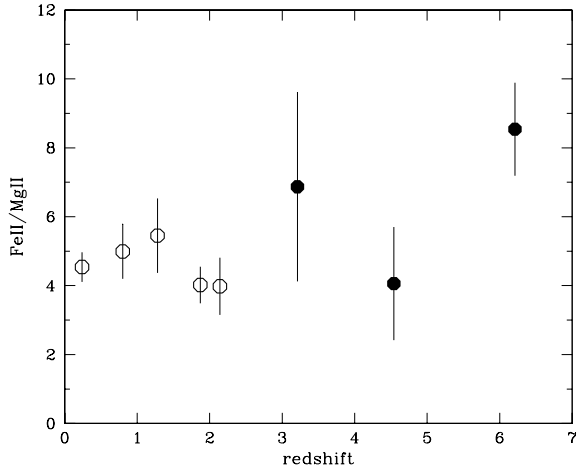

FIG. 3.— Filled symbols show the average of FeII/MgII ratios of the quasars in our three main redshift bins. Hollow symbols show the FeII/MgII ratio obtained by Dietrich et al. (2003) from optical composite spectra of quasars at lower redshift.

4. DISCUSSION

Some evidence for iron super-solar abundance was found by Wills, Netzer, & Wills (1985) in low to intermediate redshift quasars. In our spectra we detect iron emission also in all high redshift quasars. The ratio of FeII/MgII is nearly constant over the redshift range zero to 6.4. The analysis of the high redshift quasars indicate a possible increase in the FeII/MgII ratio at redshifts $z \sim 6$. If the FeII/MgII flux ratio is tracing the Fe/α abundance ratio, this result would imply that the iron abundance is nearly constant or even slightly increasing from redshift zero to 6.4, i.e. when the age of the universe was about 800 Myr. While this finding is difficult to reconcile with the scenarios ex-

pecting a delay of 1 Gyr or more for the iron enrichment, models of rapid and strong star formation at high redshift offer a plausible explanation. Indeed, Matteucci & Recchi (2001) have shown that models of early formation of ellipticals, with very efficient star formation and lasting $\sim$0.4 Gyr, imply a peak of SNIa production (hence of iron enrichment) already at 0.3 Gyr after the onset of star formation. They have also shown that in the case of an instantaneous burst the SNIa production peaks at only 50 Myr after the burst. As a consequence, our results can be explained with two possible scenarios:

1. A major episode of star formation in these highest-z quasar hosts occurred at z $\geq$ 9, to allow the estimated 0.3 Gyr required for SNIa to enrich the ISM within the context of models for star formation in elliptical hosts. The assumption that high redshift quasars are hosted in young elliptical galaxies may be reasonable, based on the studies of quasar hosts at lower redshift (Kukula et al. 2001; Dunlop et al. 2003). Nonetheless, it is also important to keep in mind that there is no direct observational evidence that these highest-z quasars reside in "normally" evolving elliptical galaxies.

2. An “instantaneous” burst of star formation occurred as late as z $\sim$ 7, and SNIa had enough time to enrich the ISM within $\sim$ 50 Myr of the burst. The ideal case of a single instantaneous burst is not likely to represent the scenario of spheroids and galaxies formation in general, for which a star formation extended in time is more plausible. However, a single instantaneous burst may have occurred in the nuclear region of these quasars, causing a rapid iron enrichment limited mostly to the central region.

It is interesting to note that the first scenario (early formation of ellipticals) implies a redshift for the first major episode of star formation (z$\geq$9) which is consistent with the redshift of the re-ionization (at z$\approx 20 \pm 10$) inferred from the recent Wilkinson Microwave Anisotropy Probe (WMAP) results (Bennett et al. 2003). While the second scenario would be more consistent with the secondary re-ionization (at z$\sim$6) proposed by Cen (2003) and Wyithe & Loeb (2003).

We also find a population of quasars at z$\sim$4.3–5.1 with low iron emission (Table 1). These objects are responsible for the apparently lower FeII bump in the average spectrum of the quasars in this redshift bin (Fig.2). Other quasars with such low Fe emission in this redshift range were also found by Dietrich et al. (2003) and by Iwamuro et al. (2002) (see also Fiore et al. 2003). Statistically we cannot make any strong statement on the fraction of quasars with low FeII. However, they could represent a population of quasars hosted in stellar systems which evolved more slowly than the quasars with higher Fe emission.

An alternative explanation for the FeII/MgII trends discussed above is that the physical conditions of the Broad Line Region in high redshift quasars are significantly different than in quasars at lower redshift. In this case the observed FeII/MgII ratio at high redshift would reflect the combined effects of abundance variations *and* variations of other physical parameters such as density, ionization parameter, and microturbulence. Disentangling these effects requires our observations to be complemented with the detection of the optical iron bump (Verner et al. 2003), which is shifted beyond the K-band at z$>$5. Observations sensitive enough to detect the optical iron bump at these redshifts will probably have to await the James Webb Space Telescope (JWST).

We thank the referee M. Dietrich for helpful comments. Part of this work was developed during the Guillermo Haro Workshop in 2003. RM acknowledges partial financial support from the Italian Space Agency (ASI). YJ and RM acknowledge support from CONACyT grant J32178-E.

REFERENCES

Aoki, K., Murayama, T., & Denda, K. 2002, PASJ, 54, 353
Baffa, C. et al. 2001, A&A, 378, 722
Barth, A., et al. 2003, to appear in ApJ, astro-ph/0308005
Bennett, C. L., et al. 2003, to appear in ApJ, astro-ph/0302207
Cen, R. 2003, ApJ, 591, 12
Dietrich, M., Appenzeller, I., Vestergaard, M., & Wagner, S. J. 2002, ApJ, 564, 581
Dietrich, M., Hamann, F., Appenzeller, I., & Vestergaard, M. 2003, to appear in ApJ, astro-ph/0306584
Dunlop, J. S., McLure, R. J., Kukula, M. J., Baum, S. A., O'Dea, C. P., & Hughes, D. H. 2003, MNRAS, 340, 1095
Fan, X. et al. 2003, AJ, 125, 1649
Fiore, F., Elvis, M., Maiolino, R., Nicastro, F., Siemiginowska, A., Stratta, G., & D'Elia, V. 2003, A&A, in press (astro-ph/0306530)
Francis, P. J., at al. 1991, ApJ, 373, 465
Freudling, W., Corbin, M. R., & Korista, K. T. 2003, ApJ, 587, L67
Greggio, L. & Renzini, A. 1983, A&A, 118, 217
Hamann, F. & Ferland, G. 1999, ARA&A, 37, 487
Iwamuro, F., Motohara, K., Maihara, T., Kimura, M., Yoshii, Y., & Doi, M. 2002, ApJ, 565, 63
Kukula, M. J., Dunlop, J. S., McLure, R. J., Miller, L., Percival, W. J., Baum, S. A., & O'Dea, C. P. 2001, MNRAS, 326, 1533
Maiolino, R., Mannucci, F., Baffa, C., Gennari, S., & Oliva, E. 2001, A&A, 372, L5
Mannucci, F. et al. 2003, A&A, 401, 519
Matteucci, F. & Recchi, S. 2001, ApJ, 558, 351
Oliva, E. 2003, Memorie della Societa Astronomica Italiana, 74, 118
Pickles, A. J. 1998, PASP, 110, 863
Thompson, K. L., Hill, G. J., & Elston, R. 1999, ApJ, 515, 487
Vanden Berk, D. E. et al. 2001, AJ, 122, 549
Verner, E., et al. 2003, to appear in ApJ, astro-ph/0306533
Vestergaard, M. & Wilkes, B. J. 2001, ApJS, 134, 1
Wills, B. J., Netzer, H., & Wills, D. 1985, ApJ, 288, 94
Wheeler, J. C., Sneden, C., & Truran, J. W. 1989, ARA&A, 27, 279
Willott, C. J., McLure, R. J., & Jarvis, M. J. 2003, ApJ, 587, L15
Wyithe, J. S. B. & Loeb, A. 2003, ApJ, 586, 693

TABLE 1
FEII/MGII MEASUREMENTS

Name	z	FeII/MgII	log λL_λ(1450Å)
BR 0019-1522	4.52	2.02±1.01	46.76
PSS J0134+3307	4.53	1.68±0.42	46.87
SDSS J021102.72-000910.3	4.73	4.10±2.05	46.17
SDSS J075618.14+410408.6	5.09	3.43±1.37	46.54
SDSS J103027.10+052455.0	6.28	8.65±2.47	46.68
SDSS J104433.04-012502.2	5.78	—[a]	46.88
SDSS J104845.05+463718.3	6.23	8.03±1.22	46.81
SDSS J114816.64+525150.3	6.40	8.20±2.10	46.98
SDSS J130608.26+035626.3	5.99	9.03±2.26	47.32
GB 6 15007+4848	3.20	4.17±0.63	47.63
BR J1603+0721	4.38	4.06±0.81	46.86
SDSS J160501.21-011220.6	4.92	5.30±1.35	46.46
PSS J1633+1411	4.35	3.23±1.28	47.02
HS 1649+3905	3.05	7.40±0.74	46.72
SDSS J173352.23+540030.5	3.42	7.74±1.16	46.99
SDSS J173744.88+582829.6	4.94	3.55±1.42	46.75
S5 1759+75	3.05	5.01±2.01	47.41
PSS J2154+0335	4.36	5.83±1.75	47.81
SDSS J220008.66+001744.8	4.77	5.50±1.65	46.56
BR 2237-0607	4.56	3.00±1.20	47.42
LBQS 2231-0015	3.02	5.77±0.86	47.06
SDSS J234625.67-001600.5	3.50	11.7±2.92	46.90

[a]The MgII of this object was not measured because it is located in the atmospheric absorption between H and K. However this quasar was used to obtain the average spectrum in Figure 2.